LRP 598/98 March 1998

Mapping of a Stochastic Magnetic Field in Toroidal Systems

O. Fischer and W.A. Cooper

Accepted for publication in
Plasma Physics Reports

Mapping of a Stochastic Magnetic Field in Toroidal Systems

O. Fischer* and W.A. Cooper
Centre de Recherches en Physique des Plasmas, Association Euratom-Confédération Suisse, Ecole Polytechnique Fédérale de Lausanne, CRPP-PPB,CH-1015 Lausanne, Switzerland

February 27, 1998

*E-mail: Olivier.Fischer@epfl.ch

Abstract

The topologic study of a stochastic magnetic field is investigated by the tracing of magnetic field lines. The first method consists of a direct integration of the field line equations. An alternative approach is to invoke the incompressibility of the magnetic field to formulate a Hamiltonian description of the magnetic field lines. The third and last approach consist to build a canonical map that models the magnetic topology. These three different methods are applied to the **TEXTOR** tokamak device with a magnetic field perturbation driven by the **D**ynamic **E**rgodic **D**ivertor (DED) coils and the results agree with respect to the extent of the island structures near the most relevant resonant surfaces. The perturbed twisted map that we have obtained differs from the standard map (radial twist map) and constitutes an efficient method for the determination of the magnetic field line trajectories.

1 Introduction

The structure of the magnetic field should, in principle, be obtained by the integration of ordinary differential equations. Magnetic fields expressed in arbitrary curvilinear coordinates such as the VMEC [1, 2, 3] coordinates (s, u, v) are often used where s parameterizes the magnetic surfaces, u (and v) is the poloidal angle (and geometric toroidal angle). A more effective approach is to regard the equations as canonical equations. In this case, the canonical coordinates are (Ψ, θ^*) (Ψ is the toroidal flux, θ^* is a poloidal coordinate) where the time is replaced by v and the Hamiltonian is χ (the poloidal flux) [4, 5, 6, 7]. With the help of the Hamiltonian, we are able to compute the map of the magnetic system. This map is computed numerically without approximations and in such way that the area is conserved. So it becomes possible to compare this map with the standard map which is most commonly used [8, 9].

The system is composed of a 3-D magnetohydrodynamic (MHD) tokamak equilibrium with finite ripple due to the discrete toroidal coils and a magnetic perturbation. The equilibrium is computed with the 3-D free boundary VMEC code. This code generates free boundary equilibria with nested magnetic flux surfaces. In this paper, we consider the **TEXTOR** tokamak device [10] to calculate equilibria and superimpose a perturbation that models the Dynamic Ergodic Divertor (DED) [10]. The magnetic field of the DED is computed using the Biot-Savart law applied to the superposition of sets of current carrying filaments.

Concerning the organization of the paper, in the first section we will introduce the equation of the magnetic field lines appropriate for field line tracing and the corresponding Hamiltonian description. We will also explain the method to compute the map. In the second section, we will examine these different methods and we shall compare the differences between the map we generate and the standard map.

2 Review of the Theory

2.1 The Equations of the Magnetic Field Lines

In general, the equations for the magnetic field lines are

$$\frac{ds}{dv} = \frac{\mathbf{B}\cdot\nabla s}{\mathbf{B}\cdot\nabla v} = \frac{B^s}{B^v}, \tag{1a}$$

$$\frac{du}{dv} = \frac{\mathbf{B}\cdot\nabla u}{\mathbf{B}\cdot\nabla v} = \frac{B^u}{B^v} \tag{1b}$$

where (s, u, v) are the VMEC curvilinear coordinates (s labels the magnetic flux, u is a poloidal coordinate and v is the geometric toroidal angle) and $\mathbf{B}$ is the sum of the equilibrium magnetic field $\mathbf{B}_e$, such that $B^s_e \equiv 0$, and the perturbation, namely,

$$\mathbf{B} = \mathbf{B}_e + \delta\mathbf{B}.$$

Without $\delta\mathbf{B}$, the magnetic field lines form nested flux surfaces [1, 4].

If we invoke the condition $\nabla\cdot\mathbf{B} \equiv 0$, we can write in a general way the magnetic field $\mathbf{B}$ as

$$\mathbf{B} = \nabla\Psi\times\nabla\theta^* + \nabla v\times\nabla\chi(\Psi,\theta^*,v) \tag{2}$$

where Ψ and χ constitute a measure of the toroidal and poloidal flux, respectively, and θ^* is a poloidal coordinate [4, 5, 6, 7]. In this case, equations (1a) and (1b) become

$$\frac{d\theta^*}{dv} = \frac{\mathbf{B}\cdot\nabla\theta^*}{\mathbf{B}\cdot\nabla v} = \frac{\partial\chi}{\partial\Psi}, \tag{3a}$$

$$\frac{d\Psi}{dv} = \frac{\mathbf{B}\cdot\nabla\Psi}{\mathbf{B}\cdot\nabla v} = -\frac{\partial\chi}{\partial\theta^*} \tag{3b}$$

from which we recognize the Hamiltonian equations with $\chi \leftrightarrow H$, $(\Psi,\theta^*) \leftrightarrow (p,q)$ and $v \leftrightarrow t$. The Hamiltonian χ can be written in the form

$$\chi(\Psi,\theta^*,v) = \underbrace{\chi_o(\Psi)}_{H_o} + \underbrace{\chi_1(\Psi,\theta^*,v)}_{H_1} \tag{4}$$

where χ_o is the contribution from the unperturbed equilibrium such that $\frac{d\chi_o}{d\Psi} = \iota(\Psi)$, and ι is the rotational transform. The calculation of the Hamiltonian and the canonical coordinates are performed numerically [4].

2.2 Calculation of the Map

Introducing new canonical variables (θ_1, θ_2) and (J_1, J_2) such $\theta_1 = \theta^*$, $\theta_2 = v$ and $J_1 = \Psi$, the Hamiltonian defined by equation (4) becomes

$$\chi(\vec{\theta}, \mathbf{J}) = \underbrace{\chi_o(J_1) + J_2}_{H_o(\mathbf{J})} + \chi_1(J_1, \theta_1, \theta_2) \tag{5}$$

and the equations of motion are

$$\frac{d\theta_1}{dt} = w_1(J_1) + \frac{\partial \chi_1}{\partial J_1}, \quad \frac{d\theta_2}{dt} = w_2 + \frac{\partial \chi_1}{\partial J_2},$$

$$\frac{dJ_1}{dt} = -\frac{\partial \chi_1}{\partial \theta_1}, \quad \frac{dJ_2}{dt} = -\frac{\partial \chi_1}{\partial \theta_2},$$

where $w_i \equiv \frac{\partial H_o}{\partial J_i}$ are the eigenfrequencies. Using the expression for H_o, we find that $w_1 = \frac{d\chi_o(J_1)}{dJ_1} \equiv \iota(J_1)$ and $w_2 = 1$. If we examine the intersections of the trajectory with the (J_1, θ_1) surface of section at $\theta_2 = constant$, the equations of motion without the perturbation define a twist mapping [11, 12]

$$J_{n+1} = J_n, \; \theta_{n+1} = \theta_n + 2\pi\alpha(J_{n+1}) \; (mod\, 2\pi) \tag{6}$$

where $\alpha = w_1/w_2$ is the rotation number, namely $\alpha = \iota$. With the perturbation introduced, we expect that equation (6) becomes

$$J_{n+1} = J_n + \epsilon f(J_{n+1}, \theta_n), \tag{7a}$$

$$\theta_{n+1} = \theta_n + 2\pi\alpha(J_{n+1}) + \epsilon g(J_{n+1}, \theta_n) \; (mod\, 2\pi), \tag{7b}$$

where the functions f and g are defined by [11]

$$f(J_{n+1}, \theta_n) \equiv -\int_0^T dt \frac{\partial \chi_1}{\partial \theta_1}(J_{n+1}, \theta_n + w_1 t, w_2 t + \theta_{20}),$$

$$g(J, \theta) \equiv -\int_0^\theta d\theta' \frac{\partial f}{\partial J}(J, \theta'),$$

and we have chosen $\theta_{20} = 0$ as an initial condition (it determines the $v = 0$ cross section). The definition of g guarantees the preservation of the area. If we introduce our Hamiltonian in these equations, we obtain

$$f(J, \theta) = -\int_0^{2\pi} dv \frac{\partial \chi_1}{\partial \theta^*}(\Psi, \theta^*, v)\Big|_{\Psi = J,\, \theta^* = \theta + \iota(\Psi)v} \tag{8a}$$

$$g(J, \theta) = -\int_0^\theta d\theta' \frac{\partial f}{\partial J}(J, \theta'). \tag{8b}$$

3 Numerical Results

The calculation for the TEXTOR equilibrium has been based on the following data: the plasma current $I_p = 346\ kA$, the major radius $R = 1.75\ m$, the minor radius $a = 0.4\ m$, the resonant $\iota = 1/3$ is located at $r = 0.38\ m$ and the resonant $\iota = 2/5$ is located at $r = 0.35\ m$. The rotational transform profile of the equilibrium is shown in Fig. 1. The DED coils are aligned to approximately coincide with the pitch of the field lines on the $\iota = 1/3$ rational surface [10]. The coil arrangement consists of 16 helical conductors carrying a current I_j, $j = 1, ...16$. We model the current I_j as a simple trigonometric function,

$$I_j = cc * I_0 sin((j-1)\pi/4 + \Omega t)$$

with $I_0 = 7.5\ kA, cc = 0.3, \Omega t = \pi/4$. Consequently the perturbed fields generated by the DED coils have a structure dominated by the $m = 6, n = 2$ component where m (n) is the poloidal (toroidal) mode number.

To compare the differences between equations (1a)-(1b), (3a)-(3b) and (7a)-(7b), we have traced the trajectories for the same initial conditions and we have plotted the result in the (s, u) plane. Thus we have had to invert $(\Psi, \theta^*) \rightarrow (s, u)$ [4]. In Fig. 2a, we have concentrated on a field line in the neighbourhood of the $\iota = 2/5$ resonant surface. A set of five island structures are observed. The field tracing method (circles), the Hamiltonian method (squares) and the canonical mapping (triangles) are in very good agreement with respect to the radial and poloidal extent of the islands. In Fig. 2b, a similar calculation is performed in the neighbourhood of the $\iota = 1/3$ resonant surface; the three island structures are more localized poloidally. The canonical mapping method yields more accurate results than the Hamiltonian approach in this case. Concerning the entire phase space, Fig. 2c shows that the field lines between the six island structures at $s \sim 0.9$ are stochastic.

In Figs. 3a and 3b, we show the behaviour of the functions f and g as a function of θ on two different field lines close to the $\iota = 1/3$ and $\iota = 2/5$ resonant surfaces. The modulation of f and g with respect to θ is due to the presence of the DED. This modulation localizes f and g in the region $1.25 \leq \theta \leq 3.76$ *radians* which corresponds to the inboard side of the TEXTOR device.

With respect to the difference between our map and the standard map, we observe that:

- f depends both on θ and J.

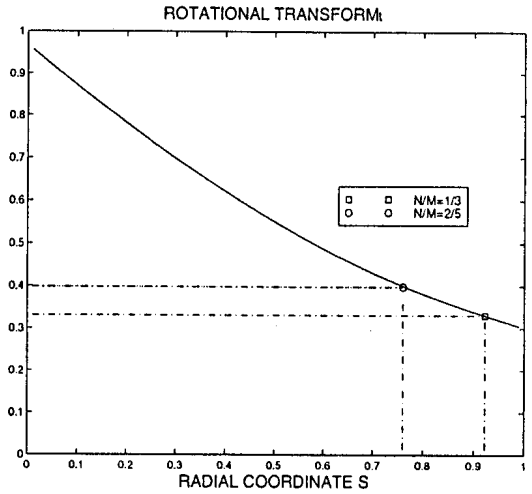

Figure 1: Rotational transform ι profile of the VMEC equilibrium as a function of s.

- The map is not a radial twist mapping, because the function g is nonvanishing.
- The function f is not a strictly simple trigonometric sine function as in the standard map ($f_{standard} \sim \sin(\theta)$), but has a more complicated spectrum ($f(J,\theta) = a_o(J)/\sqrt{2\pi} + 1/\sqrt{\pi}\sum_n a_n(J)\cos(n\theta) + b_n(J)\sin(n\theta)$). The functions $a_n(J)$ and $b_n(J)$ are displayed in Figs. 3c and 3d, respectively, as a function of J.

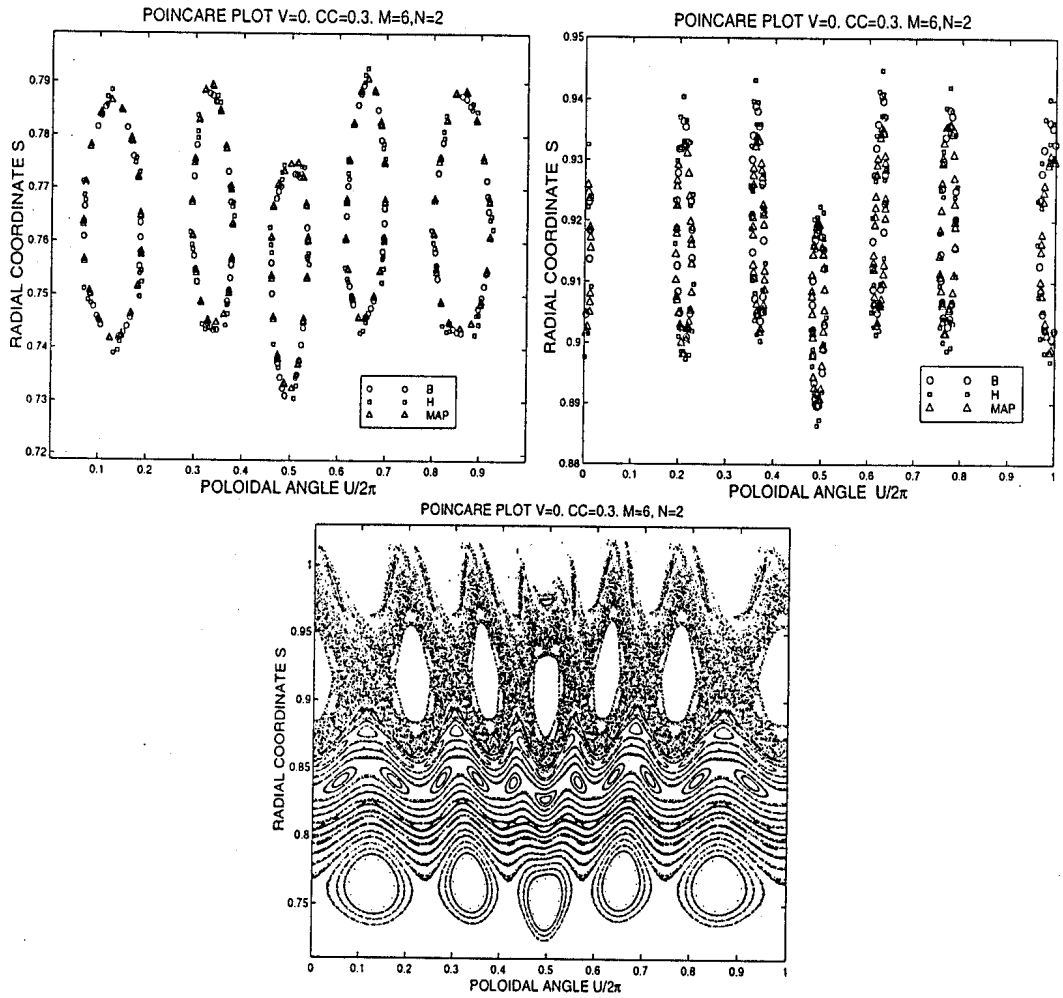

Figure 2: a) Trajectories in (s, u) coordinates on $\iota = 2/5$ surface (top left) and b) $\iota = 1/3$ (top right) (Circles: resolution with equations (1a)-(1b). Squares: resolution with equations (3a)-(3b). Triangles: resolution with equations (7a)-(7b)). c) Poincaré plot calculated with equations (1a)-(1b) in (s, u) coordinates on different surfaces (bottom).

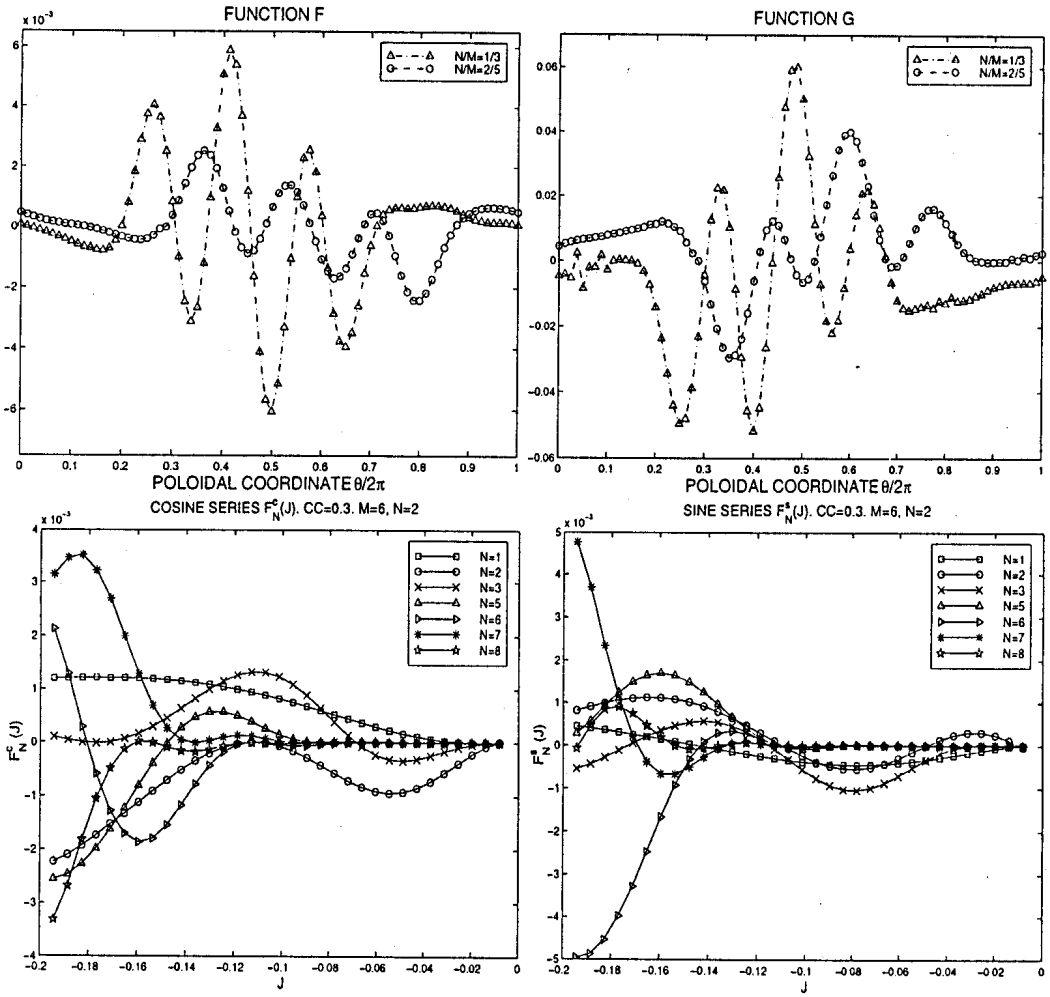

Figure 3: a) The functions $f(\theta)$ equation (8a) (top left) and b) $g(\theta)$ equation (8b) (top right) as a function of θ for different values of ι (Circles: $\iota = 2/5$. Triangles: $\iota = 1/3$). Fourier decomposition of the function f: c) cosine series component (bottom left) and d) sine series component (bottom right) as a function of J.

4 Conclusion

We have compared three different methods to determine the trajectories of magnetic field lines. An application to the TEXTOR device with activated DED coils shows very good agreement between these methods.

We have shown that the construction of a map describing the magnetic topology is possible without any approximations. We are able to compare this map with the standard map and we have seen it is not a radial twist mapping, but a perturbed twist map. Moreover, the construction of this map is independent of the system (Tokamak, Stellarators, etc.). The only restriction imposed is that the unperturbed equilibrium state should have nested magnetic flux surfaces.

The power of this canonical mapping method is that allows the treatment of complex nonlinear dynamical systems from which we can extract the functions f and g that may be fitted with analytic functions [11]. Finally, the construction of the functions f and g guarantees the conservation of area. This is not the case if we integrate the equation of motion (equations (1a)-(1b) or (3a)-(3b)) over one single period. Concerning the computational time, it takes about ten minutes to compute the Hamiltonian and about the same time for the calculation of the functions f and g on an *Indigo2 R10000*. Finally, it takes about three seconds to make one thousand iterations with equations (7a)-(7b).

ACKNOWLEDGMENTS

We acknowledge a useful discussion with Prof. H. Kunz. We thank Dr. S.P. Hirshman for providing us with the VMEC code and Dr. K.H. Finken and Dr. A. Nicolai for the input of the DED. This work was partially sponsored by the Fonds National Suisse de la Recherche Scientifique and by Euratom.

References

[1] Hirshman S P and Whitson J C 1983 *Phys. Fluids* **26** 3553

[2] Hirshman S P and Merkel P 1986 *Comput. Phys. Commun.* **43** 143

[3] Merkel P 1986 *J. Comput. Phys.* **66** 83

[4] Fischer O and Cooper W A 1997 submitted to *Plasma Phys. and Controlled Fusion*

[5] Boozer A H 1983 *Phys. Fluids* **26** 1288

[6] D'Haeseleer W D *et al.* 1991 *Flux Coordinates and Magnetic Field Structure*, (New York: Springer-Verlag)

[7] Kuo-Petravic G and Boozer A H 1987 *J. Comput. Phys.* **73** 107

[8] Horton W and Ichikawa Y H 1996 *Chaos and Structures in Nonlinear Plasmas*, (Singapore: World Scientific Publishing Co Pte Ltd)

[9] Misguich J H, Balescu R, Reuss J D, Elskens Y 1997 *Motion in a Sochastic Layer Described by Symbolic Dynamics*, Association Euratom-CEA-1605

[10] Finken K H (Ed) 1996 *The Dynamic Ergodic Divertor (DED) for TEXTOR*, Rep. Jül-3285, Kernforschungszentrum Jülich

[11] Lichtenberg A J and Lieberman M A 1992 *Applied mathematical sciences* **38**, (New York: Springer-Verlag)

[12] Meiss J D 1992 *Reviews of Modern Physics* **64** 795